

Second-order two-temperature model of heat transfer processes in a thin metal film subjected to an ultrashort laser pulse

E. MAJCHRZAK, J. DZIATKIEWICZ

*Institute of Computational Mechanics and Engineering, Silesian University of Technology, 44-100 Gliwice, Konarskiego 18a, Poland,
e-mails: ewa.majchrzak@polsl.pl, jolanta.dziatkiewicz@polsl.pl*

THERMAL PROCESSES IN DOMAIN of thin metal film subjected to an ultrashort laser pulse are considered. A mathematical description of the process discussed is based on the system of four equations. Two of them describe the electrons and lattice temperature, while third and fourth equations represent the generalized Fourier law, it means the dependencies between the electrons (lattice) heat flux and the electrons (lattice) temperature gradient. In the generalized Fourier law the heat fluxes are delayed in relation to the temperature gradients which consequently causes the appearance of heat fluxes time derivatives in the appropriate equations. Depending on the order of the generalized Fourier law expansion into the Taylor series, the first- and the second-order model can be obtained. In contrast to the commonly used first-order model, here the second-order two-temperature model is proposed. The problem is solved using the implicit scheme of the finite difference method. The examples of computations are also presented. It turns out that for the low laser intensities the results obtained using the first- and the second-order models are very similar.

Key words: thin metal films, laser heating, two-temperature model, FDM.

Copyright © 2019 by IPPT PAN, Warszawa

1. Introduction

THE TWO-TEMPERATURE MODEL DESCRIBES the temporal and spatial evolution of the lattice and electrons temperatures in the irradiated metal by two coupled nonlinear differential equations [1–7]

$$(1.1) \quad C_e(T_e) \frac{\partial T_e(X, t)}{\partial t} = -\nabla \cdot \mathbf{q}_e(X, t) - G(T_e, T_l)[T_e(X, t) - T_l(X, t)] + Q(X, t)$$

and

$$(1.2) \quad C_l(T_l) \frac{\partial T_l(X, t)}{\partial t} = -\nabla \cdot \mathbf{q}_l(X, t) + G(T_e, T_l)[T_e(X, t) - T_l(X, t)],$$

where $T_e(X, t)$, $T_l(X, t)$ are the temperatures of electrons and lattice, respectively, $C_e(T_e)$, $C_l(T_l)$ are the volumetric specific heats, $G(T_e, T_l)$ is the electron-

phonon coupling factor which characterizes the energy exchange between electrons and phonons, $Q(X, t)$ is the source function associated with the laser irradiation, X and t denote spatial co-ordinates and time. It should be pointed out that for pure metals, the incident radiation is absorbed mainly by electrons, therefore the source function $Q(X, t)$ appears only in Eq. (1.1) [8].

The two-temperature model proposed by ANISIMOV *et al.* [1] contains two additional equations based on the Fourier law describing the dependencies between electron and lattice heat fluxes and temperature gradients

$$(1.3) \quad \mathbf{q}_e(X, t) = -\lambda_e(T_e, T_l) \nabla T_e(X, t)$$

and

$$(1.4) \quad \mathbf{q}_l(X, t) = -\lambda_l(T_l) \nabla T_l(X, t),$$

where $\lambda_e(T_e, T_l)$, $\lambda_l(T_l)$ are the thermal conductivities of electrons and lattice, respectively. This model is also known as a parabolic two-step model.

QIU and TIEN [9] proposed a more general relationships between heat fluxes and temperature gradients, namely

$$(1.5) \quad \mathbf{q}_e(X, t + \tau_e) = -\lambda_e(T_e, T_l) \nabla T_e(X, t)$$

and

$$(1.6) \quad \mathbf{q}_l(X, t + \tau_l) = -\lambda_l(T_l) \nabla T_l(X, t),$$

where τ_e is the relaxation time of free electrons in metals (the mean time for electrons to change their states), τ_l is the relaxation time in phonon collisions. In this way a hyperbolic two-temperature model is obtained.

Now, the problems related to the parameters appearing in Eqs. (1.1)–(1.6) are discussed. The electron volumetric specific heat can be calculated as the derivative of the total electron energy U_e with respect to the electron temperature T_e [2, 4, 6]

$$(1.7) \quad C_e(T_e) = \frac{\partial U_e}{\partial T_e} = \int_0^{\infty} \frac{\partial f(E, \mu(T_e), T_e)}{\partial T_e} g(E) E dE,$$

where $f(E, \mu(T_e), T_e)$ is the Fermi distribution function, $g(E)$ is the electron density of states (DOS) at the energy level E , $\mu(T_e)$ is the chemical potential at the temperature T_e . It should be noted that the electron density of states can be determined from the electronic structure calculations performed within the density functional theory [2]. Determination of $C_e(T_e)$ is still not easy because the

evaluation of $\partial f/\partial T_e$ requires the knowledge of a chemical potential as a function of electrons temperature $\mu(T_e)$. Therefore, at the low electron temperatures the Sommerfeld expansion is commonly used [4] which leads to the following formula

$$(1.8) \quad C_e(T_e) = \gamma T_e,$$

where

$$(1.9) \quad \gamma = \frac{\pi^2 k_B^2 N}{2T_F},$$

while N is the electrons concentration, k_B is the Boltzmann constant and T_F is the Fermi temperature.

The electrons thermal conductivity in metals is described by the Drude model [4]

$$(1.10) \quad \lambda_e(T_e, T_l) = \frac{1}{3} C_e(T_e) \tau_e(T_e, T_l) v_e^2,$$

where $\tau_e(T_e, T_l)$ is the total electron scattering time and v_e is the mean velocity of the electrons. It is assumed that all electrons within the metal travel at the Fermi velocity, it means $v_e = v_F$. Electrons collisions can occur with other electrons, the lattice, defects, grain boundaries and surfaces. Assuming that each mechanism is independent, the Matthiessen rule [4] can be applied

$$(1.11) \quad \frac{1}{\tau_e} = \frac{1}{\tau_{ee}} + \frac{1}{\tau_{eph}} + \frac{1}{\tau_{ed}} + \frac{1}{\tau_{eb}},$$

where τ_{ee} is the electron-electron scattering time, τ_{eph} is the electron-phonon scattering time, τ_{ed} is the electron-defect scattering time and τ_{eb} is the electron-boundary scattering time.

Electron-defect and electron-boundary scattering times are both typically independent of temperature. The electron-phonon scattering time depends on the lattice temperature T_l , while the electron-electron scattering time depends on the electrons temperature. For temperatures above the Debye temperature the electron-electron scattering time in comparison with the electron-phonon scattering time can be neglected [4] and then

$$(1.12) \quad \frac{1}{\tau_e} = \frac{1}{\tau_{eph}} = B T_l,$$

where B is assumed to be constant.

Taking into account the dependencies (1.8) and (1.12) the electrons thermal conductivity (1.10) can be expressed as

$$(1.13) \quad \lambda_e(T_e, T_l) = \lambda_0 \frac{T_e}{T_l},$$

where λ_0 is the material constant (thermal conductivity in the thermal equilibrium [11]).

The volumetric specific heat of lattice can be calculated as the derivative of the total phonon energy U_l with respect to the lattice temperature T_l [5, 6]

$$(1.14) \quad C_l = \frac{\partial U_l}{\partial T_l} = \int_{\omega_1}^{\omega_2} g_l(\omega) \frac{\partial f_{BE}(\omega, T_l)}{\partial T_l} \hbar \omega d\omega,$$

where $f_{BE}(\omega, T_l)$ is the Bose–Einstein distribution function, $g_l(\omega)$ is the phonon density of states at the frequency ω , ω_1 and ω_2 are the minimum and maximum frequency of the phonons, respectively, \hbar is Planck’s constant divided by 2π .

Applying the Debye model [5, 6], under the assumption that the lattice temperature T_l is much higher than the Debye temperature T_D , the volumetric specific heat of lattice is a constant value

$$(1.15) \quad C_l = 3N_a k_B,$$

where N_a is the number of atoms per unitary volume.

The lattice thermal conductivity can be expressed as [6]

$$(1.16) \quad \lambda_l(T_l) = \frac{1}{3} C_l(T_l) \tau_{ph}(T_l) v_l^2,$$

where $\tau_{ph}(T_l)$ is the total scattering time and v_l is the phonons velocity.

Phonons collisions can occur with other phonons and defects. Using the Matthiessen rule [4, 5, 6] one obtains

$$(1.17) \quad \frac{1}{\tau_{ph}} = \frac{1}{\tau_{ph\,ph}} + \frac{1}{\tau_{ph\,d}},$$

where $\tau_{ph\,ph}$ and $\tau_{ph\,d}$ are the phonon-phonon scattering time and phonon-defect scattering time, respectively. If the temperature T_l is much higher than the Debye temperature, scattering times are not dependent on temperature. They are assumed as a constant values. For the constant value of the volumetric specific heat of lattice and $v_l = c$, where c is the speed of sound in the material, the thermal conductivity of lattice is also a constant value $\lambda_l = \lambda_0$, where λ_0 is the thermal conductivity for $T_e = T_l$ and equal to room temperature [11].

Another key parameter in the two-temperature models is the coupling factor, which for high electrons temperature can be calculated as follows [2, 4]

$$(1.18) \quad G(T_e) = \frac{G_0}{g^2(E_F)} \int_{-\infty}^{\infty} g^2(E) \left(-\frac{\partial f(E, \mu, T_e)}{\partial E} \right) dE,$$

where G_0 is the constant and E_F is the Fermi energy.

As shown in [2], for low electrons temperature ($T_e < 5000$ K) the formulas (1.8), (1.13) can be used, while the other parameters (thermal conductivity of lattice, volumetric specific heat of lattice, coupling factor) can be assumed as the constant values. In this paper, the low intensity of the laser is considered, therefore such parameter values are accepted.

We are now returning to the considerations related to the two-temperature model. Thus, the left sides of the dependencies (1.5), (1.6) are expanded into a Taylor series

$$(1.19) \quad \mathbf{q}_e(X, t) + \tau_e \frac{\partial \mathbf{q}_e(X, t)}{\partial t} + \frac{\tau_e^2}{2} \frac{\partial^2 \mathbf{q}_e(X, t)}{\partial t^2} + \dots = -\lambda_e(T_e, T_l) \nabla T_e(X, t)$$

and

$$(1.20) \quad \mathbf{q}_l(X, t) + \tau_l \frac{\partial \mathbf{q}_l(X, t)}{\partial t} + \frac{\tau_l^2}{2} \frac{\partial^2 \mathbf{q}_l(X, t)}{\partial t^2} + \dots = -\lambda_l(T_l) \nabla T_l(X, t).$$

Taking into account the first two components of this expansion one obtains the hyperbolic two-temperature model, that can be called the first-order two-temperature model.

It should be noted that the parabolic model and the first-order hyperbolic two-temperature model are widely used for numerical modeling of thermal processes occurring in the laser treated materials, e.g. [10–19].

At this point, the Maxwell–Cattaneo–Vernotte (MCV) model and the dual-phase lag (DPL) model are worth mentioning [3–6, 20–23]. These models can be derived in several ways. They belong to the so-called one-temperature models describing the macroscopic lattice temperature [3] and can be obtained, among others, from the hyperbolic two-temperature model [3] (but under the certain assumptions). It should be emphasized that the non-physical solutions can be obtained using hyperbolic models, too. These problems are analyzed by many researches, who propose the appropriate constitutive assumptions using the extended irreversible thermodynamics [24–29].

In the paper the second-order hyperbolic two-temperature model is proposed, it means in the dependencies (1.19), (1.20) three components of the Taylor expansion are taken into account. According to the best knowledge of the authors, such a model has not yet been considered. In the Section 2 the formulation of the analyzed problem is presented, Section 3 is devoted to the method of solution, while Section 4 contains the results of computations. Conclusions resulting from the comparison of the first- and second-order hyperbolic two-temperature models are formulated in the final part of the paper.

2. Formulation of the problem

Thin metal film of the thickness L (1D problem) subjected to the laser pulse is considered. For low laser intensities the relationships (1.8), (1.13) describing the electrons thermal conductivity and volumetric specific heat are widely used [13, 15, 16, 19]. Additionally the coupling factor G , thermal conductivity λ_l and volumetric specific heat C_l are assumed to be the constant values.

The second-order two-temperature model consists of the following equations

$$(2.1) \quad C_e(T_e) \frac{\partial T_e(x, t)}{\partial t} = -\frac{\partial q_e(x, t)}{\partial x} - G[T_e(x, t) - T_l(x, t)] + Q(x, t),$$

$$(2.2) \quad C_l \frac{\partial T_l(x, t)}{\partial t} = -\frac{\partial q_l(x, t)}{\partial x} + G[T_e(x, t) - T_l(x, t)],$$

$$(2.3) \quad q_e(x, t) + \tau_e \frac{\partial q_e(x, t)}{\partial t} + \frac{\tau_e^2}{2} \frac{\partial^2 q_e(x, t)}{\partial t^2} = -\lambda_e(T_e, T_l) \frac{\partial T_e(x, t)}{\partial x},$$

$$(2.4) \quad q_l(x, t) + \tau_l \frac{\partial q_l(x, t)}{\partial t} + \frac{\tau_l^2}{2} \frac{\partial^2 q_l(x, t)}{\partial t^2} = -\lambda_l \frac{\partial T_l(x, t)}{\partial x}.$$

The source function $Q(x, t)$ is associated with the laser irradiation [15, 16, 19]

$$(2.5) \quad Q(x, t) = \sqrt{\frac{\beta}{\pi}} \frac{1-R}{t_p \delta} I_0 \exp\left[-\frac{x}{\delta} - \beta \frac{(t-2t_p)^2}{t_p^2}\right],$$

where I_0 is the laser intensity, t_p is the characteristic time of laser pulse, δ is the optical penetration depth, R is the reflectivity of the irradiated surface and $\beta = 4 \ln 2$.

For $x = 0$ and $x = L$ the non-flux conditions are assumed (the external heat flux resulting from the laser action is taken into account by the introduction of the function $Q(x, t)$). The initial condition $T_e(x, 0) = T_l(x, 0) = T_p$ is also known.

3. Method of solution

To solve the problem formulated the algorithm based on the finite difference method is proposed. Thus, the staggered grid is introduced [12, 15], as shown in Fig. 1. It should be noted that this type of spatial discretization is also called the scheme of shifted fields [30], in which the spatial locations of temperature values are shifted by a space step h with respect to locations of heat flux values.

Let us denote $T_i^f = T(ih, f\Delta t)$, where h is the mesh step, Δt is the time step, $i=0, 2, 4, \dots, n$, $f=0, 1, 2, \dots, F$, and $q_j^f = q(jh, f\Delta t)$, where $j=1, 3, \dots, n-1$.

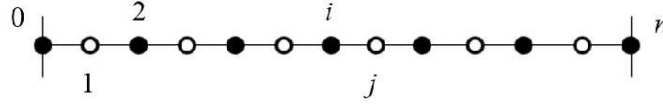


FIG. 1. Staggered grid: $i = 0, 2, 4, \dots, n$ - 'temperature nodes', $j = 1, 3, 5, \dots, n - 1$ - 'heat fluxes nodes'.

The finite difference approximation of Eqs. (2.3) and (2.4) using implicit scheme can be written in the form

$$(3.1) \quad q_{ej}^f + \tau_e \frac{q_{ej}^f - q_{ej}^{f-1}}{\Delta t} + \frac{p\tau_e^2}{2} \frac{q_{ej}^f - 2q_{ej}^{f-1} + q_{ej}^{f-2}}{(\Delta t)^2} = -\lambda_{ej}^{f-1} \frac{T_{ej+1}^f - T_{ej-1}^f}{2h}$$

and

$$(3.2) \quad q_{lj}^f + \tau_l \frac{q_{lj}^f - q_{lj}^{f-1}}{\Delta t} + \frac{p\tau_l^2}{2} \frac{q_{lj}^f - 2q_{lj}^{f-1} + q_{lj}^{f-2}}{(\Delta t)^2} = -\lambda_l \frac{T_{lj+1}^f - T_{lj-1}^f}{2h},$$

where index j corresponds to the 'heat flux nodes' (Fig. 1). For the second-order model parameter $p = 1$, while for the first-order model $p = 0$.

From Eqs. (3.1) and (3.2) it follows that

$$(3.3) \quad q_{ej}^f = -\frac{(\lambda_{ej-1}^{f-1} + \lambda_{ej+1}^{f-1})(\Delta t)^2}{2hB_e} (T_{ej+1}^f - T_{ej-1}^f) + \frac{2\tau_e(\Delta t + p\tau_e)}{B_e} q_{ej}^{f-1} - \frac{p\tau_e^2}{B_e} q_{ej}^{f-2}$$

and

$$(3.4) \quad q_{lj}^f = -\frac{\lambda_l}{hB_l} (T_{lj+1}^f - T_{lj-1}^f) + \frac{2\tau_l(\Delta t + p\tau_l)}{B_l} q_{lj}^{f-1} - \frac{p\tau_l^2}{B_l} q_{lj}^{f-2},$$

where

$$(3.5) \quad B_e = 2(\Delta t)^2 + 2\tau_e\Delta t + p\tau_e^2, \quad B_l = 2(\Delta t)^2 + 2\tau_l\Delta t + p\tau_l^2.$$

The dependencies (3.3), (3.4) allow to construct the similar formulas for nodes $i - 1, i + 1$ and then one obtains

$$(3.6) \quad q_{ei-1}^f - q_{ei+1}^f = \frac{(\lambda_{ei-2}^{f-1} + \lambda_{ei}^{f-1})(\Delta t)^2}{2hB_e} (T_{ei-2}^f - T_{ei}^f) + \frac{(\lambda_{ei+2}^{f-1} + \lambda_{ei}^{f-1})(\Delta t)^2}{2hB_e} (T_{ei+2}^f - T_{ei}^f) + \frac{2\tau_e(\Delta t + p\tau_e)}{B_e} (q_{ei-1}^{f-1} - q_{ei+1}^{f-1}) - \frac{p\tau_e^2}{B_e} (q_{ei-1}^{f-2} - q_{ei+1}^{f-2})$$

and

$$(3.7) \quad q_{li-1}^f - q_{li+1}^f = \frac{\lambda_l(\Delta t)^2}{hB_l}(T_{li-2}^f - T_{li}^f) + \frac{\lambda_l(\Delta t)^2}{hB_l}(T_{li+2}^f - T_{li}^f) \\ + \frac{2\tau_l(\Delta t + p\tau_l)}{B_l}(q_{li-1}^{f-1} - q_{li+1}^{f-1}) - \frac{p\tau_l^2}{B_l}(q_{li-1}^{f-2} - q_{li+1}^{f-2}).$$

Now, Eqs. (2.1), (2.2) are discretized using the implicit scheme of the finite difference method

$$(3.8) \quad C_{ei}^{f-1} \frac{T_{ei}^f - T_{ei}^{f-1}}{\Delta t} = -\frac{q_{ei+1}^f - q_{ei-1}^f}{2h} - G(T_{ei}^f - T_{li}^f) + Q_i^f,$$

$$(3.9) \quad C_l \frac{T_{li}^f - T_{li}^{f-1}}{\Delta t} = -\frac{q_{li+1}^f - q_{li-1}^f}{2h} + G(T_{ei}^{f-1} - T_{li}^{f-1}),$$

where index i corresponds to the 'temperature nodes', as shown in Fig. 1. Putting (3.6) into (3.8) one has

$$(3.10) \quad T_{ei}^f = T_{ei}^{f-1} + A_{e1}^{f-1}(T_{ei-2}^{f-1} - T_{ei}^{f-1}) + A_{e2}^{f-1}(T_{ei+2}^{f-1} - T_{ei}^{f-1}) \\ + A_{e3}^{f-1}(q_{ei-1}^{f-1} - q_{ei+1}^{f-1}) - A_{e4}^{f-1}(q_{ei-1}^{f-2} - q_{ei+1}^{f-2}) \\ - \frac{\Delta t G}{C_{ei}^{f-1}} T_{ei}^f + \frac{\Delta t G}{C_{ei}^{f-1}} T_{li}^f + \frac{\Delta t Q_i^f}{C_{ei}^{f-1}},$$

where

$$(3.11) \quad A_{e1}^{f-1} = \frac{(\lambda_{ei-2}^{f-1} + \lambda_{ei}^{f-1})(\Delta t)^3}{4h^2 C_{ei}^{f-1} B_e}, \quad A_{e2}^{f-1} = \frac{(\lambda_{ei+2}^{f-1} + \lambda_{ei}^{f-1})(\Delta t)^3}{4h^2 C_{ei}^{f-1} B_e}, \\ A_{e3}^{f-1} = \frac{\tau_e \Delta t (\Delta t + p\tau_e)}{h C_{ei}^{f-1} B_e}, \quad A_{e4}^{f-1} = \frac{p\tau_e^2 \Delta t}{2h C_{ei}^{f-1} B_e}.$$

From Eq. (3.10) it follows that

$$(3.12) \quad T_{ei}^f = \frac{A_{e1}^{f-1}}{A_{e5}^{f-1}} T_{ei-2}^f + \frac{A_{e2}^{f-1}}{A_{e5}^{f-1}} T_{ei+2}^f + \frac{1}{A_{e5}^{f-1}} T_{ei}^{f-1} + \frac{A_{e3}^{f-1}}{A_{e5}^{f-1}} (q_{ei-1}^{f-1} - q_{ei+1}^{f-1}) \\ - \frac{A_{e4}^{f-1}}{A_{e5}^{f-1}} (q_{ei-1}^{f-2} - q_{ei+1}^{f-2}) + \frac{\Delta t G}{C_{ei}^{f-1} A_{e5}^{f-1}} T_{li}^f + \frac{\Delta t}{C_{ei}^{f-1} A_{e5}^{f-1}} Q_i^f,$$

where

$$(3.13) \quad A_{e5}^{f-1} = 1 + A_{e1}^{f-1} + A_{e2}^{f-1} + \frac{\Delta t G}{C_{ei}^{f-1}}.$$

In a similar way one obtains (cf. Eqs. (3.7), (3.9))

$$(3.14) \quad T_{li}^f = \frac{A_{l1}}{A_{l5}} T_{li-2}^f + \frac{A_{l2}}{A_{l5}} T_{li+2}^f + \frac{1}{A_{l5}} T_{li}^{f-1} + \frac{A_{l3}}{A_{l5}} (q_{li-1}^{f-1} - q_{li+1}^{f-1}) - \frac{A_{l4}}{A_{l5}} (q_{li-1}^{f-2} - q_{li+1}^{f-2}) + \frac{\Delta t G}{C_l A_{l5}} T_{ei}^f,$$

where

$$(3.15) \quad \begin{aligned} A_{l1} &= \frac{\lambda_l (\Delta t)^3}{2h^2 C_l B_l}, & A_{l2} &= \frac{\lambda_l (\Delta t)^3}{2h^2 C_l B_l}, & A_{l3} &= \frac{\tau_l \Delta t (\Delta t + p\tau_l)}{h C_l B_l}, \\ A_{l4} &= \frac{p\tau_l^2 \Delta t}{2h C_l B_l}, & A_{l5} &= 1 + A_{l1} + A_{l2} + \frac{\Delta t G}{C_l}. \end{aligned}$$

The non-flux conditions take a form

$$(3.16) \quad \begin{aligned} x = 0 : \quad \frac{\partial T_e}{\partial x} = 0, & \quad x = L : \quad \frac{\partial T_e}{\partial x} = 0, \\ x = L : \quad \frac{\partial T_l}{\partial x} = 0, & \quad x = L : \quad \frac{\partial T_l}{\partial x} = 0 \end{aligned}$$

and the following finite difference approximation is used

$$(3.17) \quad \begin{aligned} x = 0 : \quad \frac{T_{e2}^f - T_{e0}^f}{2h} = 0, & \quad x = L : \quad \frac{T_{en}^f - T_{en-2}^f}{2h} = 0, \\ x = L : \quad \frac{T_{l2}^f - T_{l0}^f}{2h} = 0, & \quad x = L : \quad \frac{T_{ln}^f - T_{ln-2}^f}{2h} = 0, \end{aligned}$$

or

$$(3.18) \quad T_{e0}^f = T_{e2}^f, \quad T_{en}^f = T_{en-2}^f, \quad T_{l0}^f = T_{l2}^f, \quad T_{ln}^f = T_{ln-2}^f.$$

Thus, for each transition $t^{f-1} \rightarrow t^f$ the system of Eqs. (3.3), (3.4), (3.12), (3.14) supplemented by boundary conditions (3.18) should be solved using e.g. the Gauss-Seidel iterative method.

4. Results of computations

Thin metal film of the thickness 200 nm and the initial temperature distribution $T_e(x, 0) = T_l(x, 0) = 300$ K is considered. Three different materials, namely lead, titanium and vanadium are taken into account. In Table 1 the thermophysical parameters of materials are collected. The melting temperature T_m is also given. It should be pointed out, that the phase transitions are not considered here. The melting point for individual materials is given to control the calculation whether the lattice temperature does not exceed the melting point.

Table 1. Thermophysical parameters [2, 8, 31].

	Pb	Ti	V
λ_0 [W/(m · K)] (see also formula (1.13))	71.6	21.9	30.7
γ [J/(m ³ · K ²)] (formula (1.8))	748.1	328.9	67.1
C_l [J/(m ³ · K)]	$2.7417 \cdot 10^6$	$2.34 \cdot 10^6$	$2.9939 \cdot 10^6$
G [W/(m ³ · K)]	$109 \cdot 10^{16}$	$130 \cdot 10^{16}$	$523 \cdot 10^{16}$
τ_e [ps]	0.005	0.001	0.002
τ_l [ps]	0.4	0.05	0.06
T_m [K]	600.5	1941	2183

It is assumed that the laser intensity equals $I_0 = 200$ J/m² and the characteristic time of laser pulse is equal to $t_p = 0.1$ ps (reflectivity $R = 0.93$ and optical penetration depth $\delta = 15.3$ nm).

The problem is solved using the implicit scheme of the finite difference method for $n = 300$ and $\Delta t = 0.0005$ ps. For these values of n and Δt the results are grid independent.

In Figs. 2, 3 and 4 the temperature histories of electrons and lattice at the irradiated surface for the materials considered are shown. As it can be seen, depending on the material, the maximum electron temperatures are reached at the different times. In addition, the time after which the temperature of electrons and the lattice is equalized, is also different – the longest for lead (about 1.6 ps) and the shortest for vanadium (about 0.34 ps).

The results obtained using the second-order and first-order two-temperature models are compared. It turns out that the differences between the solutions are

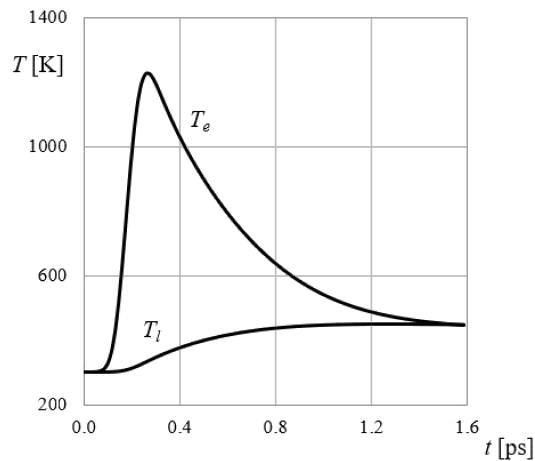


FIG. 2. Temperature histories at the irradiated surface, Pb.

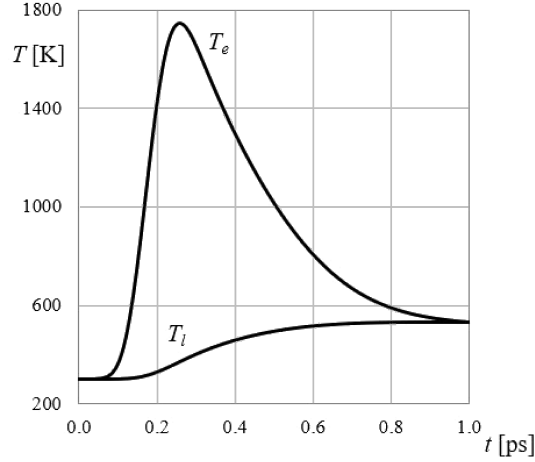


FIG. 3. Temperature histories at the irradiated surface, Ti.

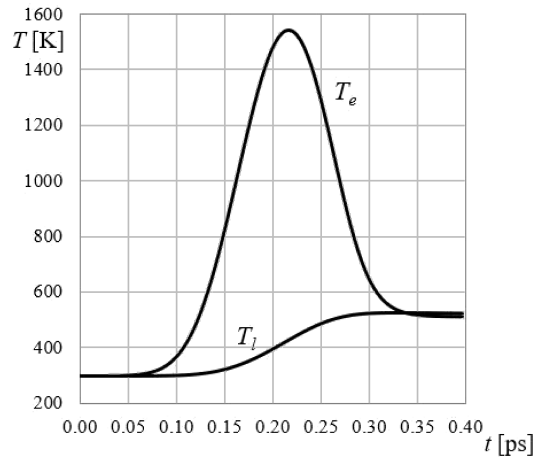


FIG. 4. Temperature histories at the irradiated surface, V.

very small. For example, in the case of lead the maximum electrons temperatures are equal to 1229.77 K and 1229.90 K, respectively, while maximum lattice temperatures are equal to 375.38 K and 375.12 K, respectively. For titanium, maximum electrons temperatures: 1744.06 K and 1744.07 K, maximum lattice temperatures: 457.20 K and 457.17 K. For vanadium: 1540.98 K, 1541.06 K and 523.63 K, 523.44 K.

The computations are repeated for other laser parameters, namely $I_0 = 400 \text{ J/m}^2$ and $t_p = 0.1 \text{ ps}$, $I_0 = 200 \text{ J/m}^2$ and $t_p = 0.05 \text{ ps}$, $I_0 = 400 \text{ J/m}^2$ and $t_p = 0.05 \text{ ps}$. In all cases, the differences between maximum electrons tem-

peratures and the maximum lattice temperatures do not exceed 0.5 K. Even for a high laser intensity e.g. $I_0 = 1800 \text{ J/m}^2$ ($t_p = 0.1 \text{ ps}$) and the vanadium thin film, when the maximum lattice temperature is close to the melting point, the differences between the second-order and first-order models are small: maximum electrons temperatures: 7905.14 K and 7905.31 K, maximum lattice temperatures: 2130.03 K and 2129.57 K.

One can see, that using the second-order two-temperature model, the electrons temperature is slightly lower in comparison with the first-order one, while the lattice temperature is slightly higher.

To compare the results of calculations with the results presented in [32], the computations are performed for a layer with the thickness $L = 100 \text{ nm}$ made of chromium. The authors of this article use the parabolic two-temperature model, thus in Eqs. (2.3), (2.4) the values $\tau_e = 0$, $\tau_l = 0$ are assumed. The following parameters of laser are accepted (formula (2.5)): intensity $I_0 = 559 \text{ J/m}^2$ and characteristic time $t_p = 0.03 \text{ ps}$. The thermophysical parameters of chromium are taken from [32].

In Fig. 5 the temperature histories of electrons and lattice at the irradiated surface are shown. The good agreement with the results presented in [32] is observed (symbols). Moreover, the time after which the temperature of electrons and the lattice is equalized, is also similar: about 4 ps.

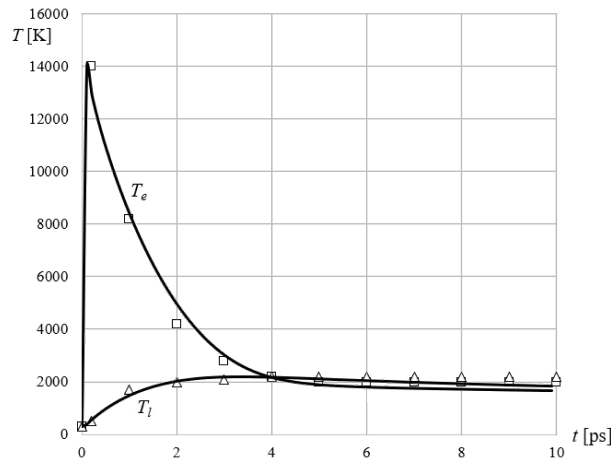


FIG. 5. Temperature histories at the irradiated surface, Cr ($I_0 = 559 \text{ J/m}^2$, $t_p = 0.03 \text{ ps}$), symbols – solution presented in [32].

Experimental research presented in the paper [32] concern the identification of laser intensity I_0 (under the assumption that the characteristic time of laser pulse is equal to $t_p = 0.03 \text{ ps}$) ensuring the achievement of melting point on

the irradiated surface of the metal film. For the laser intensity $I_0 = 559 \text{ J/m}^2$ the lattice temperature for $x = 0$ reaches the value 2180.45 K very close to the melting temperature $T_m = 2180.15 \text{ K}$.

In this paper, the thermodynamics problems [20–23] related to the second-order two-temperature model are not considered. It should be noted that using the model presented here, the physical anomalies can take place but in our calculations we have not encountered a solution that would be incorrect from a physical point of view.

5. Conclusions

The second-order two-temperature model has been presented. The problem has been solved using the implicit scheme of the finite difference method. The computations have been performed for thin metal films (lead, titanium and vanadium) subjected to the ultrashort laser pulse. Different laser parameters have been taken into account. The comparison of results obtained using the first- and second- two-temperature models show that the differences between the solutions are very small. In conclusion, the first-order two-temperature model is sufficiently accurate for the numerical modelling of thermal processes occurring in heated thin metal films. The introduction of the higher-order expansion into the Taylor series seems in this situation unnecessary.

Acknowledgements

The paper and research are financed within the project 2015/19/B/ST8/01101 sponsored by the National Science Centre (Poland).

References

1. S.I. ANISIMOV, B.L. KAPELIOVICH, T.L. PEREL'MAN, *Electron emission from metal surfaces exposed to ultrashort laser pulses*, Soviet Journal of Experimental and Theoretical Physics, **66**, 776–781, 1974.
2. Z. LIN, L.V. ZHIGILEI, V.CELLI, *Electron-phonon coupling and electron heat capacity of metals under conditions of strong electron-phonon nonequilibrium*, Physical Review B, **77**, 075133-1-0.75133-17, 2008.
3. D.Y. TZOU, *Macro- to Microscale Heat Transfer. The Lagging Behavior*, Taylor and Francis, Oxfordshire, UK, 1997.
4. Z.M. ZHANG, *Nano/Microscale Heat Transfer*, McGraw-Hill, New York, 2007.
5. A.N. SMITH, P.M. NORRIS, [in:] *Heat Transfer Handbook*, Adrian Bejan [ed.], John Wiley & Sons, Hoboken, pp. 1309–1409, 2003.

6. G. CHEN, D. BORCA-TASCIUC, R.G. YANG, [in:] *Encyclopedia of Nanoscience and Nanotechnology*; Hari Singh Nalwa [ed.], American Scientific Publishers: Stevenson Ranch, **7**, 429–459, 2004.
7. S.L. SOBOLEV, *Nonlocal two-temperature model: application to heat transport in metals irradiated by ultrashort laser pulses*, International Journal of Heat and Mass Transfer, **94**, 138–144, 2016.
8. M.A. AL-NIMR, *Heat transfer mechanisms during short-duration laser heating of thin metal films*, International Journal of Thermophysics, **18**, 5, 1257–1268, 1997.
9. T.Q. QIU, C.L. TIEN, *Heat transfer mechanisms during short-pulse laser heating of metals*, Journal of Heat Transfer, **115**, 835–841, 1993.
10. J.K. CHEN, W.P. LATHAM, J.E. BERAUN, *The role of electron–phonon coupling in ultrafast laser heating*, Journal of Laser Applications, **17**, 1, 63–68, 2005.
11. J.K. CHEN, D.Y. TZOU, J.E. BERAUN, *A semiclassical two-temperature model for ultrafast laser heating*, International Journal of Heat and Mass Transfer, **49**, 307–316, 2006.
12. H. WANG, W. DAI, R. MELNIK, *A finite difference method for studying thermal deformation in a double-layered thin film exposed to ultrashort pulsed lasers*, International Journal of Thermal Sciences, **45**, 1179–1196, 2006.
13. T. NIU, W. DAI, *A hyperbolic two-step model based finite difference scheme for studying thermal deformation in a double-layered thin film exposed to ultrashort-pulsed lasers*, International Journal of Thermal Sciences, **48**, 1, 34–49, 2009.
14. K. BAHETI, J. HUANG, J.K. CHEN, Y. ZHANG, *An axisymmetric interfacial tracking model for melting and resolidification in a thin metal film irradiated by ultrashort pulse lasers*, International Journal of Thermal Sciences, **50**, 25–35, 2011.
15. J. DZIATKIEWICZ, W. KUS, E. MAJCHRZAK, T. BURCZYNSKI, L. TURCHAN, *Bioinspired identification of parameters in microscale heat transfer*, International Journal for Multiscale Computational Engineering, **12**, 1, 79–89, 2014.
16. E. MAJCHRZAK, J. DZIATKIEWICZ, *Analysis of ultrashort laser pulse interactions with metal films using a two-temperature model*, Journal of Applied Mathematics and Computational Mechanics, **14**, 2, 31–39, 2015.
17. W. KUS, J. DZIATKIEWICZ, *Multicriteria identification of parameters in microscale heat transfer*, International Journal of Numerical Methods for Heat & Fluid Flow, **27**, 3, 587–597, 2017.
18. E. MAJCHRZAK, J. DZIATKIEWICZ, L. TURCHAN, *Analysis of thermal processes occurring in the microdomain subjected to the ultrashort laser pulse using the axisymmetric two-temperature model*, International Journal for Multiscale Computational Engineering, **15**, 5, 395–411, 2017.
19. J.K. CHEN, J.E. BERAUN, *Numerical study of ultrashort laser pulse interactions with metal films*, Numerical Heat Transfer, Part A, **40**, 1–20, 2001.
20. A. SELLITTO, V.A. CIMMELLI, D. JOU, *Nonequilibrium thermodynamics and heat transport at nanoscale*, [in:] Mesoscopic Theories of Heat Transport in Nanosystems, pp. 1–30, Springer International Publishing, Lausanne, 2016.
21. R. KOVÁCS, P. VÁN, *Generalized heat conduction in heat pulse experiments*, International Journal of Heat and Mass Transfer, **83**, 613–620, 2015.

22. W. DREYER, H. STRUCHTRUP, *Heat pulse experiments revisited*, Continuum Mechanics and Thermodynamics, **5**, 3–50, 1993.
23. I. MÜLLER, T. RUGGERI, *Rational Extended Thermodynamics*, Springer, Oklahoma, 1998.
24. S.A. RUKOLAINE, *Unphysical effects of the dual-phase-lag model of heat conduction*, International Journal of Heat and Mass Transfer, **78**, 58–63, 2014.
25. S.A. RUKOLAINE, *Unphysical effects of the dual-phase-lag model of heat conduction: higher-order approximations*, International Journal of Thermal Sciences, **113**, 83–88, 2017.
26. M. FABRIZIO, B. LAZZARI, V. TIBULLO, *Stability and thermodynamic restrictions for a dual phase-lag thermal model*, Journal of Non-Equilibrium Thermodynamics, **42**, 3, 243–252, 2017.
27. R. KOVÁCS, P. VÁN, *Thermodynamical consistency of the dual-phase-lag heat conduction equation*, Continuum Mechanics and Thermodynamics, **30**, 6, 1223–1230, 2017.
28. M. FABRIZIO, F. FRANCHI, *Delayed thermal models: stability and thermodynamics*, Journal of Thermal Stresses, **37**, 2, 160–173, 2014.
29. R. QUINTANILLA, R. RACKE, *Qualitative aspects in dual-phase-lag heat conduction*, Proceedings of the Royal Society of London, A: Mathematical, Physical and Engineering Sciences, **463**, 2079, 659–674, 2007.
30. Á. RIETH, R. KOVÁCS, T. FÜLÖP, *Implicit numerical schemes for generalized heat conduction equations*, International Journal of Heat and Mass Transfer, **126**, 1177–1182, 2018.
31. E. KANNATTEY-ASIBU JR., *Principles of laser materials processing*, John Wiley & Sons, Inc., Hoboken, New Jersey, 2009.
32. M. SAGHEBFAR, M.K. TEHRANI, S.M.R. DARBANI, A.E. MAJD, *Femtosecond pulse laser ablation of chromium: experimental results and two-temperature model simulations*, Applied Physics A, **123**, 28, 1–10, 2017.

Received November 25, 2018; revised version March 27, 2019.

Published online May 27, 2019.
